

# Towards clinically translatable NIR fluorescence molecular guidance for colonoscopy

P. Beatriz Garcia-Allende,<sup>1,\*</sup> Jürgen Glatz,<sup>1</sup> Maximilian Koch,<sup>1</sup> Jolien J. Tjalma,<sup>2</sup> Elmire Hartmans,<sup>2</sup> Anton G.T. Terwisscha van Scheltinga,<sup>3</sup> Panagiotis Symvoulidis,<sup>1</sup> Gooitzen M. van Dam,<sup>2</sup> Wouter B. Nagengast,<sup>2</sup> Vasilis Ntziachristos<sup>1</sup>

<sup>1</sup>Chair for Biological Imaging & Institute for Biological and Medical Imaging, Technische Universität München and Helmholtz Zentrum München, Trogerstr. 9 D-81675, München, Germany

<sup>2</sup>Dept. of Gastroenterology and Hepatology, UMCG, Hanzeplein 1, 9700 RB, Groningen, Netherlands

<sup>3</sup>Dept. of Hospital and Clinical Pharmacy, UMCG University of Groningen, Hanzeplein 1, 9700 RB, Groningen, Netherlands

\*pb.garcia-allende@helmholtz-muenchen.de

**Abstract:** White-light surveillance colonoscopy is the standard of care for the detection and removal of premalignant lesions to prevent colorectal cancer, and the main screening recommendation following treatment for recurrence detection. However, it lacks sufficient diagnostic yield, exhibits unacceptable adenoma miss-rates and is not capable of revealing functional and morphological information of the detected lesions. Fluorescence molecular guidance in the near-infrared (NIR) is expected to have outstanding relevance regarding early lesion detection and heterogeneity characterization within and among lesions in these interventional procedures. Thereby, superficial and sub-surface tissue biomarkers can be optimally visualized due to a minimization of tissue attenuation and autofluorescence by comparison with the visible, which simultaneously enhance tissue penetration and assure minimal background. At present, this potential is challenged by the difficulty associated with the clinical propagation of disease-specific contrast agents and the absence of a commercially available endoscope that is capable of acquiring wide-field, NIR fluorescence at video-rates. We propose two alternative flexible endoscopic fluorescence imaging methods, each based on a CE certified commercial, clinical grade endoscope, and the employment of an approved monoclonal antibody labeled with a clinically applicable NIR fluorophore. Pre-clinical validation of these two strategies that aim at bridging NIR fluorescence molecular guidance to clinical translation is demonstrated in this study.

©2013 Optical Society of America

**OCIS codes:** (170.2150) Endoscopic imaging; (170.2680) Gastrointestinal.

## References and links

1. L. Herszényi and Z. Tulassay, "Epidemiology of gastrointestinal and liver tumors," *Eur. Rev. Med. Pharmacol. Sci.* **14**(4), 249–258 (2010).
2. S. Misale, R. Yaeger, S. Hobor, E. Scala, M. Janakiraman, D. Liska, E. Valtorta, R. Schiavo, M. Buscarino, G. Siravegna, K. Bencardino, A. Cercek, C. T. Chen, S. Veronese, C. Zanon, A. Sartore-Bianchi, M. Gambacorta, M. Gallicchio, E. Vakiani, V. Boscaro, E. Medico, M. Weiser, S. Siena, F. Di Nicolantonio, D. Solit, and A. Bardelli, "Emergence of KRAS mutations and acquired resistance to anti-EGFR therapy in colorectal cancer," *Nature* **486**(7404), 532–536 (2012).
3. T. E. Goranova, M. Ohue, Y. Shimoharu, and K. Kato, "Dynamics of cancer cell subpopulations in primary and metastatic colorectal tumors," *Clin. Exp. Metastasis* **28**(5), 427–435 (2011).
4. S. E. Baldus, K. L. Schaefer, R. Engers, D. Hartleb, N. H. Stoecklein, and H. E. Gabbert, "Prevalence and heterogeneity of KRAS, BRAF, and PIK3CA mutations in primary colorectal adenocarcinomas and their corresponding metastases," *Clin. Cancer Res.* **16**(3), 790–799 (2010).

5. E. M. Stoffel, D. K. Turgeon, D. H. Stockwell, L. Zhao, D. P. Normolle, M. K. Tuck, R. S. Bresalier, N. E. Marcon, J. A. Baron, M. T. Ruffin, D. E. Brenner, and S. Syngal; Great Lakes-New England Clinical Epidemiology and Validation Center of the Early Detection Research Network, "Missed adenomas during colonoscopic surveillance in individuals with Lynch syndrome (hereditary nonpolyposis colorectal cancer)," *Cancer Prev. Res. (Phila.)* **1**(6), 470–475 (2008).
6. L. M. Wong Kee Song, D. G. Adler, B. Chand, J. D. Conway, J. M. B. Croffie, J. A. Disario, D. S. Mishkin, R. J. Shah, L. Somogyi, W. M. Tierney, and B. T. Petersen; ASGE Technology Committee, "Chromoendoscopy," *Gastrointest. Endosc.* **66**(4), 639–649 (2007).
7. L. M. W. K. Song, D. G. Adler, J. D. Conway, D. L. Diehl, F. A. Farraye, S. V. Kantsevov, R. Kwon, P. Mamula, B. Rodriguez, R. J. Shah, and W. M. Tierney; ASGE Technology Committee, "Narrow band imaging and multiband imaging," *Gastrointest. Endosc.* **67**(4), 581–589 (2008).
8. L. M. W. K. Song, S. Banerjee, D. Desilets, D. L. Diehl, F. A. Farraye, V. Kaul, S. R. Kethu, R. S. Kwon, P. Mamula, M. C. Pedrosa, S. A. Rodriguez, and W. M. Tierney; ASGE Technology Committee, "Autofluorescence imaging," *Gastrointest. Endosc.* **73**(4), 647–650 (2011).
9. R. Banerjee and D. N. Reddy, "Advances in endoscopic imaging: Advantages and limitations," *J. Dig. Endosc.* **3**(5), 7–12 (2012).
10. T. Ahmed, J. Monti, and B. Lashner, "Random versus targeted biopsies for colorectal cancer surveillance in inflammatory bowel disease," *Gastroenterol. Hepatol.* **6**(7), 438–442 (2010).
11. S. A. Hilderbrand and R. Weissleder, "Near-infrared fluorescence: application to *in vivo* molecular imaging," *Curr. Opin. Chem. Biol.* **14**(1), 71–79 (2010).
12. P. L. Hsiung, J. Hardy, S. Friedland, R. Soetikno, C. B. Du, A. P. Wu, P. Sahbaie, J. M. Crawford, A. W. Lowe, C. H. Contag, and T. D. Wang, "Detection of colonic dysplasia *in vivo* using a targeted heptapeptide and confocal microendoscopy," *Nat. Med.* **14**(4), 454–458 (2008).
13. M. V. Marshall, D. Draney, E. M. Sevick-Muraca, and D. M. Olive, "Single-dose intravenous toxicity study of IRDye 800CW in Sprague-Dawley rats," *Mol. Imaging Biol.* **12**(6), 583–594 (2010).
14. A. G. Terwisscha van Scheltinga, G. M. van Dam, W. B. Nagengast, V. Ntziachristos, H. Hollema, J. L. Herek, C. P. Schröder, J. G. Kosterink, M. N. Lub-de Hoog, and E. G. de Vries, "Intraoperative near-infrared fluorescence tumor imaging with vascular endothelial growth factor and human epidermal growth factor receptor 2 targeting antibodies," *J. Nucl. Med.* **52**(11), 1778–1785 (2011).
15. E. J. Blok, P. J. K. Kuppen, J. E. M. van Leeuwen, and C. F. M. Sier, "Cytoplasmic overexpression of HER2: a key factor in colorectal cancer," *Clin. Med. Insights Oncol.* **7**, 41–51 (2013).
16. M. Goetz, M. S. Hoetker, M. Diken, P. R. Galle, and R. Kiesslich, "In vivo molecular imaging with cetuximab, an anti-EGFR antibody, for prediction of response in xenograft models of human colorectal cancer," *Endoscopy* **45**(6), 469–477 (2013).
17. W. Scheuer, G. M. van Dam, M. Dobosz, M. Schwaiger, and V. Ntziachristos, "Drug-based optical agents: Infiltrating clinics at lower risk," *Sci. Transl. Med.* **4**, 134ps11 (2012).
18. E. M. Sevick-Muraca, W. J. Akers, B. P. Joshi, G. D. Luker, C. S. Cutler, L. J. Marnett, C. H. Contag, T. D. Wang, and A. Azhdarinia, "Advancing the translation of optical imaging agents for clinical imaging," *Biomed. Opt. Express* **4**(1), 160–170 (2013).
19. Z. Liu, S. J. Miller, B. P. Joshi, and T. D. Wang, "In vivo targeting of colonic dysplasia on fluorescence endoscopy with near-infrared octapeptide," *Gut* **62**(3), 395–403 (2013).
20. N. Thekkekk, M. C. Pierce, M. H. Lee, A. D. Polydorides, R. M. Flores, S. Anandasabapathy, and R. R. Richards-Kortum, "Modular video endoscopy for *in vivo* cross-polarized and vital-dye fluorescence imaging of Barrett's-associated neoplasia," *J. Biomed. Opt.* **18**(2), 026007 (2013).
21. C. M. Lee, C. J. Engelbrecht, T. D. Soper, F. Helmchen, and E. J. Seibel, "Scanning fiber endoscopy with highly flexible, 1 mm catheterscopes for wide-field, full-color imaging," *J. Biophotonics* **3**(5-6), 385–407 (2010).
22. S. J. Miller, C. M. Lee, B. P. Joshi, A. Gaustad, E. J. Seibel, and T. D. Wang, "Targeted detection of murine colonic dysplasia *in vivo* with flexible multispectral scanning fiber endoscopy," *J. Biomed. Opt.* **17**(2), 021103 (2012).
23. J. Glatz, J. Varga, P. B. Garcia-Allende, M. Koch, F. R. Greten, and V. Ntziachristos, "Concurrent video-rate color and near-infrared fluorescence laparoscopy," *J. Biomed. Opt.* **18**(10), 101302 (2013).
24. G. van Dam, G. Themelis, L. M. Crane, N. J. Harlaar, R. G. Pleijhuis, W. Kelder, A. Sarantopoulos, J. Bart, P. S. Low, and V. Ntziachristos, "Intraoperative tumor-specific fluorescent imaging in ovarian cancer by folate receptor- $\alpha$  targeting: first in-human results," *Nat. Med.* **17**, 1315–1319 (2011).
25. J. A. Udovich, N. D. Kirkpatrick, A. Kano, A. Tanbakuchi, U. Utzinger, and A. F. Gmitro, "Spectral background and transmission characteristics of fiber optic imaging bundles," *Appl. Opt.* **47**(25), 4560–4568 (2008).
26. M. A. Funovics, R. Weissleder, and U. Mahmood, "Catheter-based *in vivo* imaging of enzyme activity and gene expression: feasibility study in mice," *Radiology* **231**(3), 659–666 (2004).
27. R. J. Shah, D. G. Adler, J. D. Conway, D. L. Diehl, F. A. Farraye, S. V. Kantsevov, R. Kwon, P. Mamula, S. Rodriguez, L. M. Wong Kee Song, and W. M. Tierney; ASGE Technology Committee, "Cholangiopancreatography," *Gastrointest. Endosc.* **68**(3), 411–421 (2008).
28. A. R. Rouse, A. Kano, J. A. Udovich, S. M. Kroto, and A. F. Gmitro, "Design and demonstration of a miniature catheter for a confocal microendoscope," *Appl. Opt.* **43**(31), 5763–5771 (2004).

29. T. J. Muldoon, M. C. Pierce, D. L. Nida, M. D. Williams, A. Gillenwater, and R. Richards-Kortum, "Subcellular-resolution molecular imaging within living tissue by fiber microendoscopy," *Opt. Express* **15**, 16413–16423 (2007).
  30. D. P. Noonan, D. S. Elson, G. P. Mylonas, A. Darzi, and G. Z. Yang, "Laser-induced fluorescence and reflected white light imaging for robot-assisted MIS," *IEEE Trans. Biomed. Eng.* **56**(3), 889–892 (2009).
  31. R. S. Bradley and M. S. Thorniley, "A review of attenuation correction techniques for tissue fluorescence," *J. R. Soc. Interface* **3**(6), 1–13 (2006).
  32. P. A. Valdés, F. Leblond, V. L. Jacobs, B. C. Wilson, K. D. Paulsen, and D. W. Roberts, "Quantitative, spectrally-resolved intraoperative fluorescence imaging," *Sci. Rep.* **2**, 798 (2012).
  33. M. Raica, A. M. Cimpean, and D. Ribatti, "Angiogenesis in pre-malignant conditions," *Eur. J. Cancer* **45**(11), 1924–1934 (2009).
  34. A. J. McEwan, H. F. Van Brocklin, and C. Divgi, "Action plan for emerging molecular imaging technologies," *J. Nucl. Med.* **49**(2), 37N–40N (2008).
  35. International Commission on Non-Ionizing Radiation Protection, "Revision of guidelines on limits of exposure to laser radiation of wavelengths between 400 nm and 1.4  $\mu\text{m}$ ," *Health Phys.* **79**(4), 431–440 (2000).
  36. P. B. Garcia-Allende, J. Glatz, M. Koch, and V. Ntziachristos, "Enriching the interventional vision of cancer with fluorescence and optoacoustic imaging," *J. Nucl. Med.* **54**(5), 664–667 (2013).
- 

## 1. Introduction

Colorectal cancer (CRC) remains the second leading cause of cancer-related deaths in the western world and is one of the most prevalent cancer types both in men and women [1]. Along these lines, the main unmet key aspects in surveillance colonoscopy, which is the current standard for the prevention and relapse screening of CRC, are early lesion detection and the identification of the tumor characteristics to determine the optimal treatment for the individual patients diagnosed with the disease. Surveillance colonoscopy procedures rely on macroscopic features such as color or texture fluctuations observed under illumination with white light, which makes the detection of small precursor lesions particularly difficult. Molecular characterization of the detected lesions, which guides the selection of new targeted treatments in oncology [2], is performed in tissue biopsies. These biopsies cannot reveal the heterogeneity of the lesions themselves and between the primary tumor and the adjacent lymph node metastases [3,4]. Consequently, and despite the wide clinical acceptance of white-light colonoscopy, its lack of sensitivity to sub-surface activity and its incapability to elucidate particular physiological and molecular disease features of the detected premalignant lesions result in substantial lesion miss-rates that can be as high as 55% in patients with an inherited predisposition to colon cancer, such as Lynch syndrome [5].

Given this inadequate diagnostic yield, namely the information available for the endoscopists to detect and differentiate lesions, high-resolution endoscopy and filter-based systems have arisen and are commercially available from several manufacturers. These advanced endoscopic methods encompass chromoendoscopy [6], narrow band imaging (NBI) [7], and autofluorescence imaging (AFI) [8]. Chromoendoscopy consists in the topical application of stains or dyes on the colonic mucosa to highlight micro-anatomical changes that remain imperceptible under white-light illumination, but its widespread use has been prevented by limitations such as its elevated time consumption, the lack of standardized classification systems and reproducibility [9]. NBI highlights hemoglobin absorption by restricting illumination to the blue and green areas of the spectrum, thus making diseased tissue appear darker than surrounding healthy mucosa. AFI detects endogenous fluorescent substances such as NADH, FAD and porphyrins [9], without the administration of exogenous fluorescent agents. Both NBI and AFI have proven reasonable sensitivity in the delineation of adenomas from surrounding non-dysplastic tissue, therefore, assisting in lesion removal, but have not improved adenoma detection [10]. These imaging modalities aim at a contrast enhancement to facilitate lesion detection. Although further studies are still required to validate their utility as stand-alone diagnostic methodologies [7], they may be undoubtedly valuable tools when used as part of a multimodal imaging scheme [8]. However, they exploit the optical contrast intrinsic to the tissue and do not confront the lack of information about the

expression of recognized disease biomarkers and the heterogeneity of such expression, which is of paramount importance to guide lesion differentiation and targeted treatment selection.

Given this scenario, there is still an unmet clinical need for an endoscopic imaging modality that can highlight flat precursor lesions, visualize below the surface, and give insight into the biological characteristics of the CRC lesions. Wide field targeted imaging with near-infrared fluorescence [11] appears to be a promising approach for a number of reasons. First, wide-field imaging is preferable to *virtual or optical biopsy* as achieved for example by confocal endomicroscopy [12], which still relies first on white-light colonoscopy for the identification of suspicious areas and it is not suited for screening large surfaces [9]. Therefore, the real clinical need, which lies in the identification at first sight and over a large area of the bowel wall of those tissue locations that require a closer look, is not solved. Secondly, the employment of NIR fluorescent agents with targeting specificity to cancer moieties simultaneously allows for the heterogeneous visualization of specific tissue biomarkers, overcomes the limitations of color imaging regarding sub-surface visualization since light tissue penetration is increased, and maximizes lesion-to-background ratio since tissue autofluorescence is reduced with respect to the visible. Thereby, substantially more information for elucidating a personalized targeted treatment is gained.

Widespread clinical use of targeted imaging with near-infrared fluorescence in colonoscopy has been, however, limited by both technological and translational hurdles. The successful development and approval of novel contrast agents is a time and cost intensive process. Prior to toxicity and efficacy studies of the agent, promising targets need to be identified through the histological characterization with respect to marker overexpression, histomorphological and molecular heterogeneity of excised adenoma and CRC lesions. We prioritize here the reduction of the risk in clinical translation and use an approved monoclonal antibody, like trastuzumab targeting epidermal growth factor receptor 2 (HER2), and clinically applicable NIR fluorophores, like IRDye 800CW, as suggested in [13]. These are not FDA approved, but are currently being used clinically in Europe (ClinicalTrials.gov number, NCT01508572). Recently, we validated the NIR fluorescent tracer trastuzumab-800CW in an animal study [14]. Although the data on HER2 expression in colorectal cancer are still ambiguous due to differences in staining/scoring techniques, further confirmation of the pathophysiological role of cytoplasmic HER2 would create a new treatment option for about 360,000 patients a year, a clear breakthrough in the treatment of colorectal cancer [15]. This molecular characterization would allow immediate patient selection, and in the case of tumor heterogeneity can potentially be used for follow-up of targeted therapy [16]. Consequently, we are putting the ease of the pathway from the bench to the clinic in a higher order of importance than the outperformance of the targeting efficacy and the biomarker expression.

Technological challenges mainly arise from the fact that current medical endoscopes are predominantly videoscopes, i.e. they utilize a small CCD chip embedded at the distal tip of the scope that has insufficient sensitivity for acquiring NIR fluorescence images in real-time, especially in microdosing concentrations, which is currently one of the main guidelines to try to overcome regulatory barriers in the clinical propagation of novel (nuclear and optical) imaging agents engineered to be disease-specific [17,18]. In the case of monoclonal antibodies, because of the larger molecular weight, the maximum dose considered is  $\leq 30$  nanomoles [17]. Liu et al. have proposed an *in vivo* fluorescence imaging system based on a paediatric urethroscope to confront this issue [19]. Although it provides outstanding imaging resolution and satisfies real-time constraints, it would be more appropriate for percutaneous or intraoperative use since rigid rod lenses cannot be incorporated with the flexible endoscopes that are routinely used in gastrointestinal endoscopy. Accordingly, flexible alternatives have also been suggested. Commercial autofluorescence endoscopes incorporate two separate CCDs at their tip, and a filter that only enables tissue autofluorescence in the 500-630 nm range is placed in front of the CCD that acquires the fluorescence signal.

Sequential color and autofluorescence imaging is achieved alternating white and blue light via a rotating filter in front of the light source [8]. Similarly, the modular video endoscope reported in [20] provides white-light, cross-polarized and fluorescence imaging capabilities via an endoscope cap allocating interchangeable filter modules. Because of the minimal tissue autofluorescence in the NIR and the small quantities of the exogenous contrast agents that are administered to ease the pathway towards clinical translation, this design cannot be redefined for operating in this higher waveband in a straight forward manner. Within the same framework, a scanning approach has been implemented by Lee et al. [21,22]. It exhibits an ultra-compact coaxial-design with an outer diameter of 1.6 mm, which allows it to be guided through the working channel of routine endoscopes [21]. A single optical fiber is vibrated laterally using a custom tubular piezoelectric actuator and scans the image plane in an outwardly growing spiral pattern (frame rates of 30 and 15 Hz for 500 or 1000 line images, respectively). Additionally, both confocal and non-confocal collection methods are supported [21]. In the non-confocal geometry the backscattered light is collected by a ring of high numerical aperture (NA) multimode fibers that surround the fiber scanner, whose location, size and number determine the collection efficiency. The latest development of this scanning endoscope incorporates 12 step-index plastic optical fibers with a NA of 0.63 and outer diameter of 250  $\mu\text{m}$  [22], yet the attained sensitivity was insufficient to image fluorophore concentrations below 1  $\mu\text{M}$ . Bearing in mind the abovementioned limitation imposed by microdosing administration, more sensitive detection is required. At the expense of the image resolution, two alternative approaches using coherent fiber-optic bundles are proposed and characterized here. Both implementations make use of a previously developed camera system comprising a color camera and an electron multiplying charge couple device (EMCCD) camera for concurrent white-light and NIR fluorescence acquisition [23]. The diffuse nature and lack of anatomical landmark appearance of NIR fluorescence images makes orientation challenging for the physician. Simultaneous acquisition and co-registration of color and fluorescence image, as opposed to solutions that switch between acquisition modes, provides an easy and natural guidance that directly relates biomarker expression to the visual appearance itself.

In this study, we present an adaptation of a clinical grade gastrointestinal fiberscope for simultaneous, video-rate, color and NIR fluorescence imaging, as well as a miniaturized alternative that can be integrated with conventional medical videocolonoscopes. Both imaging platforms are compared for endoscopic use in terms of their attenuation in the NIR range, resolution and detection limit. In addition, the technique for in vivo characterization of the molecular characteristics of CRC lesions is pre-clinically validated.

## **2. Materials and methods**

### *2.1 Imaging platforms for fluorescence-guided colonoscopy*

#### *2.1.1 Wide-field, concurrent, video-rate color and NIR fluorescence flexible endoscopy*

We have initially considered a fiberscope (GIF-XQ20, Olympus, Center Valley, US-PA) to replace the common objective that was previously shared by the color and fluorescence camera in the imaging system as employed in the first clinical translation of targeted fluorescence to provide information on surgical markers [24]. The fiberscope optically transmits the images through a coherent fiber-optic bundle and is connected via a mechanical and focusing adapter to the camera system. A multi-branched fiber-optic bundle (SEDI-ATI Fibres Optiques, Courcouronnes, France) simultaneously couples white-light illumination (KI-2500 LCD, Schott AG, Mainz, Germany) and fluorescence excitation (BWF2-750-0, B&W Tek, Newark, US-DE) into the illumination port of the endoscope. The multi-branched end of the bundle consists of 4 branches (one terminated in a mechanical ferrule adapted to our white-light source and 3 with SMA connectors). Independent illumination and imaging channels are particularly suitable since background signal from the autofluorescence of the

imaging bundle is prevented [25]. Additional filters are allocated in the light path to assure that the fluorescence and white-reflectance measurements are restricted to the wavebands of interest. A more detailed description about image transfer, co-registration and display to the practitioner can be found in a previous publication [23].

### 2.1.2 Miniature flexible fluorescence endoscope

The replacement of the videoendoscopes that are routinely used in the clinics nowadays by the previous fiberscope to realize the acquisition of fluorescence images at video-rate induces a significant resolution loss in the color videos, i.e. it impedes normal clinical workflow. In light of this, an alternative implementation mainly consisting of a semi-disposable, coherent imaging bundle that is long and thin enough to be inserted through the accessory channels of routine videocolonoscopy is proposed, as suggested by Funovics et al. for shorter working lengths [26]. To satisfy our requirements regarding the number of pixel elements, the field of view, working length and distal diameter, we considered the employment of a miniaturized fiberscope (SpyGlass Direct Visualization Probe, Boston Scientific, Marlborough, US-MA) that is used routinely in *cholangiopancreatography*, which consists in the endoscopic exploration of the biliary and pancreatic ducts utilizing a miniature endoscope or *cholangioscope* [27]. The latter is during the exploration routed through the working channel of a therapeutic endoscope, which is sufficiently large to accommodate it, an approach dubbed *mother-daughter* technique. The probe consists of a 6,000 pixel image bundle surrounded by approximately 225 light transmission fibers that cover the coherent bundle as an outer sheath (similarly two channels for fiber autofluorescence minimization purposes). It has maximal diameter of 0.9 mm, a working length of 231 cm and includes a lens at the distal tip of the imaging bundle that allows image capture across a 70° field of view. Consequently, its wide field of view and reduced diameter facilitate its employment as the *babyscope* for fluorescence acquisition in a mother-daughter system where a conventional videocolonoscopy acts as the mother scope. Table 1 summarizes the technical features of the miniature endoscope by comparison with the fiberscope employed in the endoscopic imaging alternative suggested in the previous section.

**Table 1. Technical specifications of the two clinical grade scopes employed in the wide-field, concurrent, video-rate color and NIR fluorescence imaging platform for flexible endoscopy**

Manufacturer	Olympus	Boston Scientific
Model name	GIF-XQ20	Spy Glass Probe
Distal diameter (mm)	9.8	0.77
Accessory channel (mm)	2.8	No
Depth of field (mm)	3-100	2-7
Working length (mm)	1025	3000
Angulation	(Up/down) 210/90 (Left/right) 100/100	120/120
Field of view (air)	120°	70°
Number of picture elements	~20000	6000

As described in detail in our previous publication [23], the camera system uses two different cameras operating in parallel. Color videos are recorded using a Pixelfly qe, PCO AG (Kelheim, Germany), with a resolution of 1.3MPixel and a pixel size of 6.45 x 6.45 μm, while the camera dedicated to fluorescence video acquisition (Andor, DU-897, Andor Technology, Belfast, Northern Ireland) has 512 x 512 active pixels with a corresponding size of 16 x 16 μm. In a like manner to custom developments used by others in fluorescence confocal microscopy [28] and microendoscopy [29,30], a custom developed zoom system was designed for magnifying the image of the proximal end of the imaging bundle to fill the dimensions of the fluorescence camera sensor. This camera choice was based on the main interest in the easy and quick characterization of the molecular characteristics of the lesions

over large fields of view using targeted fluorescent agents, while the color images would only be used to provide accurate localization and superimposition on the high resolution images from the conventional videoscope. This offers the additional advantage of ease of adaptation between intraoperative and gastrointestinal endoscopy environments, since any required modification of the earlier intraoperative version of the system is accomplished in front of the beamsplitter that separates the two image components. The zoom system is based on an infinity optical microscope design and it consists of a 40x / 0.75 NA infinity-corrected objective lens (Olympus) and an achromatic doublet with NIR AR coating to minimize the reflectivity at the fluorescence emission wavelength (AC254-100-B, Thorlabs, Newton, US-NJ). The appropriate focal length of the lens was selected to achieve a combined magnification of the objective and the lens that maximizes the area of the fiber image on the fluorescence CCD. Mechanical adapters, positioners and supports were used as needed to assure a comfortable and stable use in the endoscopy suite, while combined white-light and laser illumination is similarly provided through the multimodal light guide. In the employment in the endoscopy suite an additional shortpass filter (e.g. ET700SP, Chroma Technology, Rockingham, US-VT) would need to be placed in the white-light source of the videoendoscope to minimize tissue reflectance at the wavelengths in the range of the emission waveband to enter the fluorescence detection path. Composite Fig. 1 schematizes and compares the proposed alternatives for wide-field, video-rate, concurrent white-light and NIR fluorescence imaging in flexible endoscopy.

### 2.1.3 Attenuation in the fluorescence excitation path

The proposed imaging platforms for NIR fluorescence guidance in surveillance colonoscopy are based on clinical grade fiberscopes that are employed in white-light endoscopy of the gastrointestinal tract and the biliary and pancreatic ducts, respectively. Consequently, it is expected that their transmittance is not optimized in the NIR region of the spectrum. The illumination power at the tip of both endoscopes, as well as after the multi-branched fiber-optic bundle, was measured with a power meter, as an estimation of their attenuation in this waveband, and to confirm their capability to operate with NIR fluorescent probes.

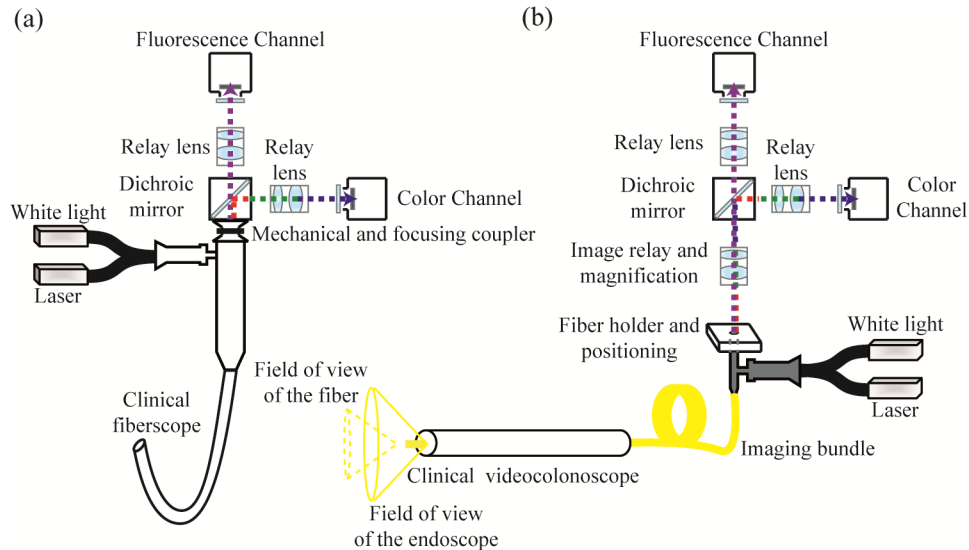


Fig. 1. Schematic of the two imaging platforms proposed for NIR fluorescence guidance in surveillance colonoscopy; (a) shows the adaption of the clinical grade gastrointestinal fiberscope, while the alternative based on the semi-disposable imaging fiber bundle that can be integrated with conventional videocoloscopes is shown in (b).

#### 2.1.4 Optical resolution measurements

The resolution of the endoscopic system was examined in the fluorescence channel to determine the minimum size of identifiable lesions. Because of the geometrical constraints of the endoscopic environment, i.e. epi-illumination and detection geometries, cross-sectional imaging is not possible. Subsequently, only the lateral resolution is characterized. To this aim the different pattern groups in a 1951 United States Air Force resolution target (USAF 1951, NT53-714, Edmund Optics, Barrington, US-NJ) were imaged. The points of the contrast transfer function (CTF) were obtained employing the Michelson contrast formula that is commonly used for patterns as the USAF 1951 and defines the contrast as the quotient between the difference and the sum of the maximum and minimum gray values of adjacent line patterns.

#### 2.1.5 Sensitivity characterization

In order to determine the system's sensitivity under typical operating conditions in the endoscopy suite and to demonstrate its capability to provide the physician with immediate feedback about the molecular characteristics of the lesions, a dilution series of IRDye 800CW (Li-Cor Biosciences, Lincoln, US-NE) phantoms was measured. Each subsequent phantom consisted of a halved concentration of the tracer labeling dissolved in phosphate buffered saline (PBS), with a total volume of 2 ml and initial concentrations of 0.20  $\mu\text{M}$  and 1.70  $\mu\text{M}$ , for the implementations based on the fiberscope and the reusable probe, respectively. The dilutions were contained in a black cylinder with a diameter of 2.54 cm and a depth of 1.27 cm, which translates to a sample thickness of 3.95 mm. Additionally, a control phantom of the same dimensions and containing only PBS was measured. The phantoms were imaged through the designed implementations at a working distance of 1 cm. Video-rate imaging at a frame-rate of 10 fps was performed by setting the fluorescence camera's exposure time to 100 ms. The acquisition parameters remained constant over the measurement series for easy comparison of signal intensities between phantoms. A region of interest (ROI) representing an active volume of about 8  $\mu\text{L}$  was selected for each measurement. The phantom concentrations correspond to an amount ranging from 1.60 pmol to 3.32 fmol and 13.60 pmol and 26.56 fmol in the active volume for the fiberscope and the reusable probe, respectively. The signal-to-noise ratio (SNR) for a fluorescence measurement was calculated as:

$$SNR_{dB} = 20 \log \left( \frac{S}{RMSN} \right) \quad (1)$$

Thereby  $S$  is the mean signal intensity in the ROI, while RMSN is the root-mean-square noise of the control image. We defined the detection limit as the concentration where the signal is three times higher than the noise, which corresponds to an SNR of 9.5 dB.

#### 2.2 Human colon cancer xenografts

Three male athymic nude mice (Harlan, Horst, The Netherlands), 16-20 weeks old, were subcutaneously inoculated with human colon tumor cell lines HCT116<sup>luc</sup> (Caliper Life Sciences, Hopkinton, US-MA). Growth of the tumors was monitored by measuring their diameter with a digital caliper, while stable transfection of the cell lines with the firefly gene *luciferase* also allowed for screening by luminescence imaging of the mice using an IVIS Spectrum (Caliper Life Sciences). HER2 positive expression of the cell surface was confirmed using fluorescence activated cell sorting (FACS). The antibody against HER2, namely trastuzumab (Herceptin®; F. Hoffmann-La Roche, Basel, Switzerland) was labeled with the NIR dye IRDye 800-CW as previously described [14], and intravenously administrated via the penile vein on the fourth week, when tumors measured approximately 6-15 mm in diameter. All experiments were performed using general anesthesia (2.5%

isoflurane in oxygen 0.4 L/min), approved by the animal welfare committee of the University of Groningen and carried out in accordance with the Dutch Animal Welfare Act of 1997.

### *2.3 Imaging data statistical analysis*

Endoscopic explorations are performed in epi-illumination and detection geometry. Consequently, the fluorescence intensity measured by the proposed imaging platforms is modulated by the tissue optical properties and the depth of the recorded activity, and does not directly report the underlying agent concentration. Although correction techniques that aim at the compensation of the effects of absorption and scattering in tissue to quantify the absolute fluorophore concentration are emerging [31,32], an overall solution to this challenge is still pending. In light of this, the tumor-to-background ratio (TBR) for the labeled antibody is estimated as the quotient of the average fluorescence intensities in the segmented lesion and a ring region-of-interest (ROI) adjacent to the tumor. Because of the fluorescence signal being diffused to the surrounding areas as a result from scattering, this approach might result in estimated TBRs being significantly smaller than if a non-tumorous region away from the lesion was selected. It tries, however, to minimize the variation of the tissue optical properties between selected areas.

## **3. Results**

### *3.1 Performance of the endoscopic imaging platforms*

#### 3.1.1 Illumination power for fluorescence excitation

While the maximum output power of the continuous wave laser diode employed in fluorescence excitation is 300 mW, a transmitted power of 243 mW at 750 nm was measured after the multi-branched randomized fiber bundle that is employed for simultaneous coupling of white-light illumination and fluorescence excitation into the illumination port of the fiberscopes. Illumination powers measured at the tip of the double channel fiber-optic bundles were 45 and 21 mW, respectively. This corresponds to a maximum attenuation of approximately 10.6 dB for the miniature endoscope and 7.3 dB for the adapted fiberscope for gastrointestinal endoscopy.

#### 3.1.2 Lateral resolution characterization

The CTF was determined from images of the USAF 1951 bar groups taken with the proposed endoscopic imaging platforms, as shown in Fig. 2 (dots). The modulus of the CTF was linearly fitted (solid line), and the line pairs corresponding to a contrast of 26.4%, applying the Rayleigh criterion, were determined to be 5 and 2 lp / mm for the clinical grade fiberscope and the miniature cholangioscope, respectively. By taking the half-width between two line pairs, it was determined that features with corresponding dimensions of 100 and 250  $\mu\text{m}$  could be resolved, demonstrating sufficient resolution for small lesion identification. As expected from the number of picture elements, resolution is considerably higher for the fiberscope GIF-XQ20, but this gain in the resolution with respect to the miniature cholangioscope that can be inserted to the accessory channel is obtained at the expense of no high resolution image available for white-light illumination.

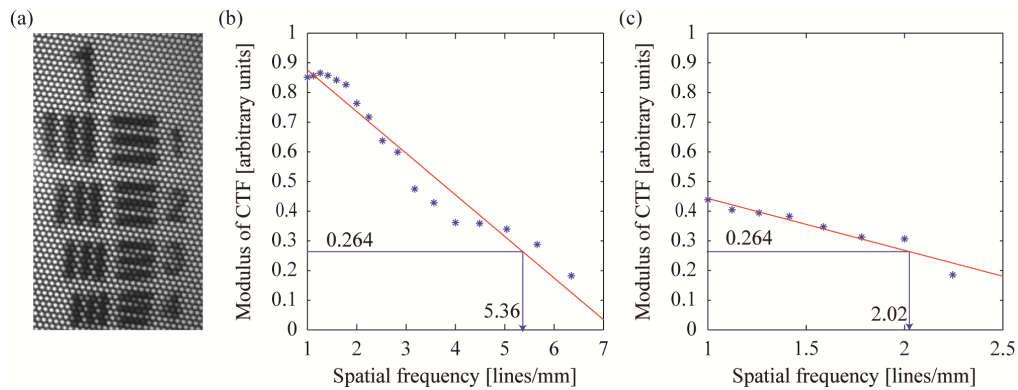


Fig. 2. (a) Detail of the USAF 1951 resolution target image. Contrast transfer functions obtained by determining the specific contrast produced by bar group patterns of various spatial frequencies taken by the endoscopic imaging platforms based on a clinical grade fiberscope (b) and on the miniature cholangioscope (c).

### 3.1.3 Sensitivity

The signal-to-noise ratio was calculated for the dilution series of IRDye 800CW, as shown in Fig. 3 for the two fiberendoscopes (dots). As expected the image quality decreases approximately linearly with the concentration. From the regression line (solid), the detection limit of 9.5 dB was calculated to lie at concentrations of 5.97 nM and 23.11 nM, which equal amounts of 47.79 fmol and 0.18 pmol in the active volume of about 8  $\mu$ L, corresponding to the selected ROI with an optical thickness of approximately 3.95 mm. The fiberscope with larger diameter and better image resolution also achieves higher sensitivity. Reported detection limits that still satisfy video-rate imaging constraints are attained through the employment of an imaging fiber bundle to relay the fluorescence images to a highly sensitive sensor module, and are expected to surpass detection capabilities of videoscopes for fluorescence imaging in the NIR, given the current state of the art CCD chips on the tip of the flexible scopes. The determined detection limits mainly represent a characteristic of the imaging setup. However, bearing in mind the previously determined tumor uptakes [14], these sensitivities are expected to be sufficient for detecting small lesions. Moreover, no significant detriment is expected to occur when imaging in tissue, since fluorescence imaging is performed in the NIR range, where influence from tissue attenuation is minimized with respect to the visible. Yet, further improvement in the detection limit could be achieved coupling additional excitation to the presently unused SMA branches of the multimodal illumination bundle.

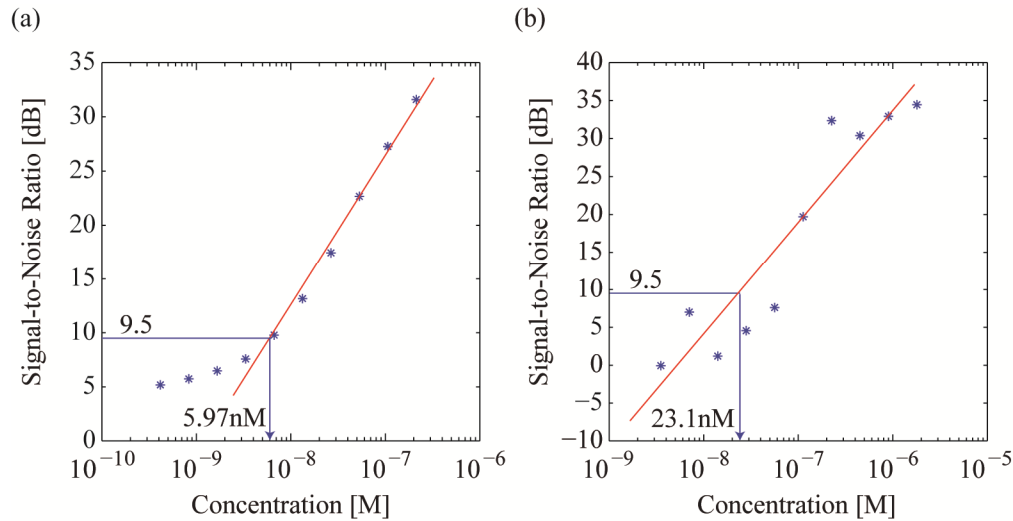


Fig. 3. Signal-to-noise ratio over concentration measured from the CW800 dilution series by the endoscopic imaging platforms based on a clinical grade fiberscope (a) and on the miniature cholangioscope (b), both under video-rate constraints (100 ms exposure time).

### 3.2 *In vivo* NIR fluorescence imaging

Representative images of the *in vivo* testing of the sensitivity of the proposed NIR fluorescence endoscopes are presented in Fig. 4. The shown images correspond to a subcutaneous colonic tumor created by inoculating human colon carcinoma cells in the left dorsal flank of the mouse. The mouse was intravenously administered with the targeted contrast agent 48 hours prior to the examination. Color and NIR fluorescence epi-illumination images were obtained with the adapted gastrointestinal endoscope (Fig. 4(a) and 4(b)) and the miniature cholangioscope (Fig. 4(d) and 4(e)) placed above the mouse. The mouse is in turn placed on a 1 cm x 1 cm grid to have an estimation of the tumor size. Gaussian filtering was applied to mitigate the visualization of the honeycomb pattern typical of fiberscopes and originating from the claddings around each fiber within the coherent imaging bundle. Coregistered color and fluorescence images are displayed both independently and superimposed (Fig. 4(c) and 4(f)) to the user by the custom designed software, while histological confirmation was performed post-mortem on tissue slides preserved from the tumor, as well as from control organs (Fig. 4(g) and Fig. 4(h)). The fluorescence images in Fig. 4(d) and 4(e) are first thresholded and then fluorescence intensities over the threshold are preserved to generate a pseudo-color overlay that is superimposed on the color images via alpha blending. Thereby, the composite images in Fig. 4(c) and 4(f) are generated. Comparison of the top and middle horizontal panels in Fig. 4 evidences the limitations of the alternative designed to be inserted through the accessory channel of conventional videoscopes, mainly regarding its low resolution, as expected from the restricted number of individual fibers that compose the coherent bundle, and its restricted depth of field. The observed fluorescence signal, which is elevated even through the skin, also suggests that its sensitivity, however, is sufficient.

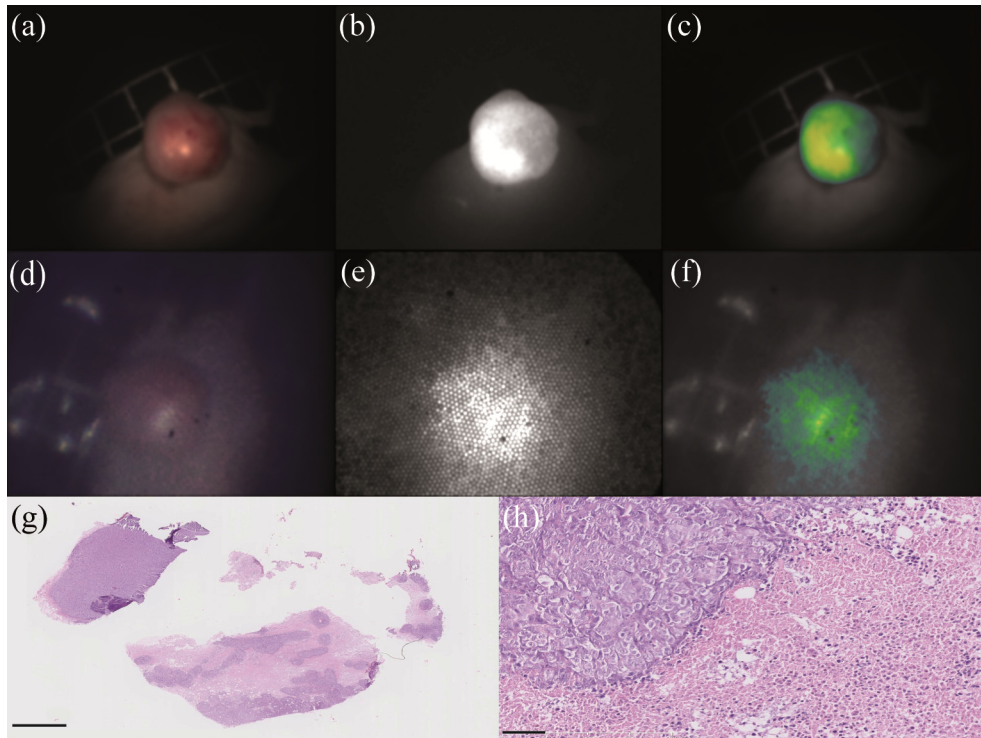


Fig. 4. Comparison of the visualization of a subcutaneous tumor with the proposed imaging platforms; Color images under white-light illumination, fluorescence and color with superimposed fluorescence acquired with the adapted fiberscope for gastrointestinal endoscopy ((a) to (c)) and the miniature cholangioscope ((d) to (f)); (g) H&E stained tissue slide preserved from the subcutaneous tumor; Scale bar 1 mm (h) Detail of H&E staining (20x); Scale bar 50  $\mu\text{m}$ .

In clinical endoscopy the endoscope is first introduced towards the proximal end of the colon, the *cecum*, and then imaging is performed while extracting the endoscope backwards. In this situation the section of the colon lumen that needs to be imaged at every instant has approximately a cylindrical shape with a diameter between 2.5 – 4 cm (depending on insufflation) and a depth of 4 – 5 cm from the tip of the endoscope. Figure 5 demonstrates the capability of the proposed approach for the minimally invasive visualization of the HER2 expression in the lesions present in this cylindrical imaged section of the colon for future human clinical studies. The adapted fiberscope for gastrointestinal endoscopy was again placed above the mouse at approximate distances of 2, 4 and 6 cm. It is important to note here the sharpness of the margins between the subcutaneous lesion and the surrounding areas, which showcases the preferential accumulation in the lesions of the targeted agent. The average TBR measured from the segmented subcutaneous lesions to the surrounding ring ROIs was  $2.69 \pm 0.27$ .

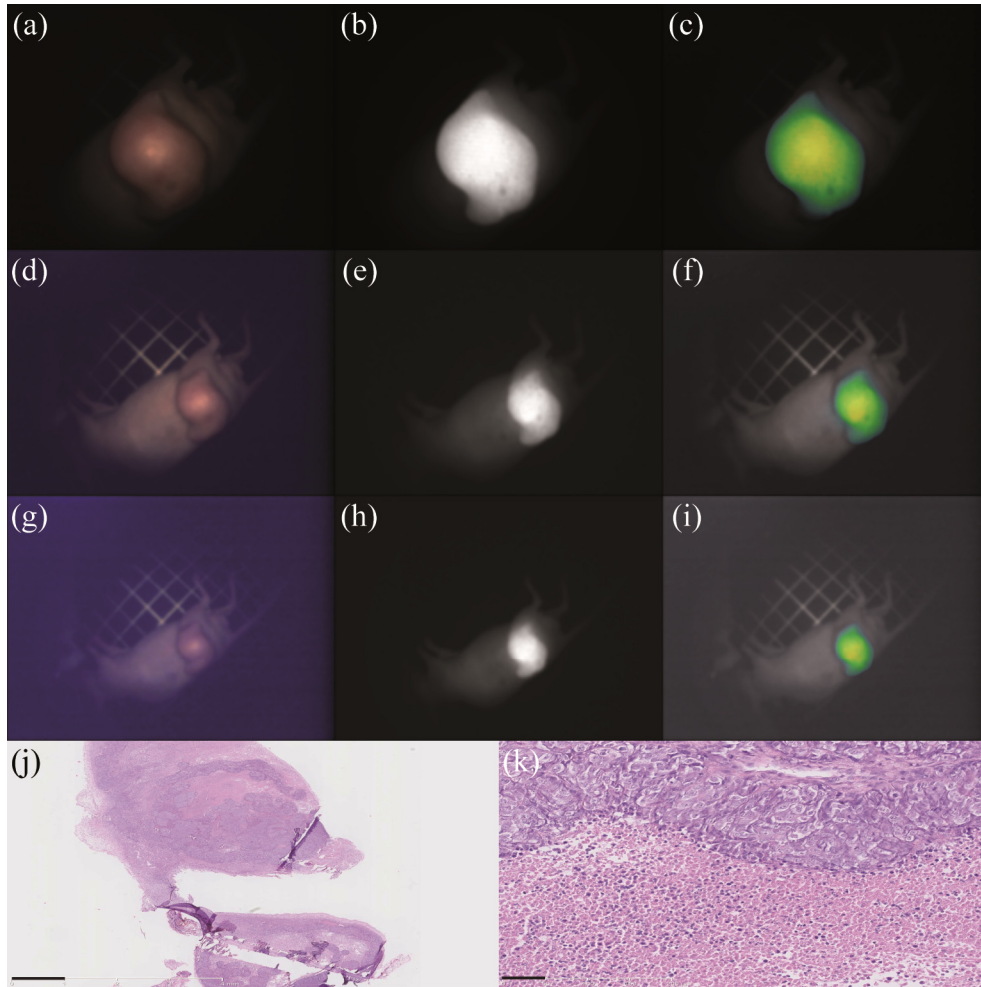


Fig. 5. Representative images that showcase the characterization of the HER2 expression in the inoculated subcutaneous tumor in 2-6 cm upfront in the bowel with an insufflation-dependent diameter; color images ((a), (d), and (g)), fluorescence ((b), (e), and (h)), and color with superimposed fluorescence ((c), (f), and (i)) were acquired with the adapted fiberscope for gastrointestinal endoscopy at 2, 4 and 6 cm distances, respectively; (j) H&E stained tissue slide preserved from the subcutaneous tumor; Scale bar 1 mm; (k) Detail of H&E staining (20x); Scale bar 50  $\mu$ m.

#### 4. Discussion and conclusions

Fluorescence molecular guidance in NIR is expected to have outstanding relevance regarding early lesion detection and revealing functional and morphological information of the detected lesions, thereby improving the diagnostic yield of surveillance colonoscopy and identifying the optimal treatment for the diagnosed patient. However, these clinical potentialities are currently prevented by the regulatory difficulties in the clinical propagation of disease-specific fluorescent agents and the lack of a commercially available flexible endoscope that is capable of acquiring simultaneous color and NIR fluorescence images at video-rates. In this study we have confronted both challenges to bridge NIR fluorescence molecular guidance to clinical translation by a straight-forward development of a technological platform and by the employment of a contrast agent based on an approved monoclonal antibody for therapy.

Regarding the minimization of the translational risk with respect to new chemical entities that have never been administered to humans, an optical agent based on a clinically approved

drug that targets a therapeutically relevant carcinoma-related biomarker, namely trastuzumab targeting HER2 was used. Specificity of binding of the labeled drug was demonstrated in subcutaneous murine tumor models and an average TBR in the NIR fluorescence channel of approximately 3 was found even when the ROI for the background was selected adjacent to the segmented lesions. The employment of an antibody targeting disease-associated human biomarkers, which is intended to enable the pathway to clinical translation in colonoscopy of the technique, prevents, however, its demonstration in an animal model of colon cancer. Future research includes the investigation of alternative mouse models, such as modified peritoneal, orthotopic and genetic tumor models to allow their visualization from inside the colon lumen. Furthermore, and although the study was focused on the visualization of biomarker expression for the identification of optimal treatments, a red-flag technique that facilitates the detection of small and precursor lesions could be based on an identical methodology, provided that alternative contrast agents targeting established biomarkers that are overexpressed in colorectal adenomas, such as bevacizumab targeting vascular endothelial growth factor (VEGF) [33], were used. Systemically administered agents may offer better lesion targeting within the entire field of view, as well as avoid spraying inhomogeneity, and provide better access to deeper seated lesions by comparison with topically sprayed fluorescent agents that are also considered as an alternative approach to reduce the translational risk for new agents. Although challenged by the difficulties in the regulatory process, it is expected that these agents benefit from the experience in nuclear medicine [34] and, thereby, are expected to find a pathway to clinical translation (ClinicalTrials.gov number, NCT01508572).

In addition, we proposed and characterized two alternative approaches to confront the insufficient sensitivity in the NIR of routine videoendoscopes. Both endoscopic imaging platforms consist in the adaptation of a gastrointestinal fiberscope and a miniature fiber-optic probe that is used in white-light endoscopy of the biliary and pancreatic ducts, respectively, for compatibility with a previously developed camera system for concurrent white-light and fluorescence acquisition. The employment of clinical grade fiberscopes to relay the fluorescence images to a more sensitive sensor module is advantageous for two reasons. First, sensitivity requirements for contrast agent visualization at microdosing administration are satisfied. Thereby, the incapability of current clinical wide-field endoscopic technologies to provide information about the expression of specific disease-associated biomarkers to guide targeted treatment selection is confronted. Based on the results from the resolution and sensitivity characterization studies, the approach would also provide a great asset for aiding in the detection of lesions that are currently easily missed in clinical endoscopy. These are protruding lesions of sizes in the order of several millimeters and flat lesions that, in spite of being sometimes as large as up to 1 cm, remain imperceptible because of the lack of contrast to the surrounding tissue. Both types of lesions are at least one order of magnitude above the size of the features that can be resolved with the proposed endoscopic imaging platforms and are expected to accumulate large amounts of the contrast agent. Secondly, their CE certification facilitates the approval for use in humans of the imaging platforms, thereby alleviating the risk for demonstrating the potential of targeted NIR fluorescence guidance. The adapted gastrointestinal fiberscope, because of its larger diameter, achieves better illumination, field of view, image resolution and sensitivity. These advantages are, however, attained at the expense of no high-definition images available for the white-light illumination either. The miniature cholangioscope was selected for the second imaging implementation because it is the only clinical grade fiberscope that is long and thin enough to be guided through the accessory channel of a conventional videocolonoscopy. The detection limit determined in the characterization stage and the levels of detected fluorescence signals suggest, however, sufficient sensitivity for *in vivo* imaging. Consequently, the approach might be adequate for providing a red-flag lesion detection strategy over a wide-field of view. Additionally, and since at typical operating distances, the power densities corresponding to

the maximum laser output at the distal tip of the endoscopes are below the limits established by the International Commission of Non-Ionizing Radiation Protection [35], further improvement in the detection limit could be achieved, either by coupling additional light sources to the remaining branches of the bifurcated fiber or improving the coupling efficiency of the mechanical connections via conventional optics or light cones or tapers.

The benefits of fluorescence imaging in the NIR have been highlighted in the accomplished preclinical validation, namely deep photon penetration, the enhancement in the tumor-to-background ratio through a minimization of the tissue autofluorescence and its easiness of integration around conventional white-light endoscopy in patient care suites since it does not overlap with normal human or color vision. In spite of this, detected fluorescence intensity, and as a consequence the characterization of the heterogeneity of the biomarker expression, is still affected by light-tissue interaction phenomena and further research is required for precise quantification of the agent uptake. Though, areas with clear positive and negative target expression can be elucidated with this approach. Another limitation is that cross-sectional imaging is not possible and, even if the fluorescence signals can be collected from depths of at least few millimeters, these appear attenuated and mixed with more superficial signals. This implies that the determined molecular information will always be surface-weighted and to address this limitation other novel imaging modalities would need to be incorporated [36].

Altogether we pre-clinically anticipated a wide-field technique based on NIR targeted fluorescence for the detection of precursor lesions of CRC and the determination of the molecular characteristics of the detected lesions. Specific binding of a monoclonal antibody labeled with IRDye 800CW to lesions overexpressing a therapeutically relevant carcinoma-related human biomarker was shown and the sensitivity of the proposed endoscopic imaging platforms was proven to be sufficient for the inspection of 0.72-6 cm upfront in the bowel with an insufflation-dependent diameter, as it is expected for the clinical application. The relevance of this endoscopic imaging modality in surveillance colonoscopy procedures will be explored in a clinical study that will commence shortly (NL-43407.042.113).

### **Acknowledgments**

This research was partially supported by a Marie Curie Intra European Fellowship within the 7th European Community Framework Program.